Pool boiling mechanisms over micro-textured surfaces

A. S. Moita[1,*], E. Teodori[1], A. L. N. Moreira[1]

1: IN+ - Department of Mechanical Engineering, Instituto Superior Técnico – TU Lisbon, Lisbon Portugal
* correspondent author: anamoita@dem.ist.utl.pt

Abstract The present work addresses a detailed study on the pool boiling processes on surfaces with a known and well defined number of artificially created cavities, to quantify the effect of the surface topography, on the interaction mechanisms. The cavities are square and have a fixed depth h_R=20μm. Special emphasis is given in how these interaction mechanisms affect bubbles dynamics and consequently the various parcels of the pool boiling heat transfer. Understanding the flow induced by the bubbles motion is vital, since Han and Griffith (1962), report that the convection induced by bubble motion may represent a relative importance of nearly 80%, comparing to the other two parcels. An innovative analysis of the boiling process from structured surfaces is proposed here, which combines image post-processing with PIV measurements. The results show that the characterization of the bubble dynamics by image analysis allows identifying optimum micro-textures which balance the effect of promoting activation of nucleation sites with a controlled activity of horizontal coalescence, thus effectively enhancing the pool boiling heat transfer. Analysis of the characteristic bubbles' velocity obtained by PIV measurements evidences that optimal patterns controlling horizontal coalescence (with a distance between cavities S=400μm) allow a more stable vertical bubble velocity, thus removing the vapour from the surface. However, the velocity of the bubbles for these surfaces is quite low, when compared to that of surfaces with a smaller number of cavities, i.e., with larger S. Hence, the convection induced by bubble motion is reduced in these optimal patterned surfaces, although the heat transfer coefficient is the highest. In line with this one may argue that the positive effect of increasing nucleation sites (under controlled coalescence) improves greatly the latent heat parcel, which is the dominant mechanism. This may be so, since the surface pattern promoting the largest velocities (C7, S=1200μm) has the lowest heat transfer coefficient, given the lowest number of active nucleation sites. Additionally, destabilization of the bubbles velocity is induced in this surface (S=1200μm), which would actually contribute to the deterioration of the heat transfer coefficient.

1. Introduction

Several thermal management strategies have been explored within the last years in the context of the cooling of electronic components. Pool boiling is a very attractive solution, given its effectiveness and its hardware simplicity. Such effectiveness is due to the particular mechanism of heat transfer which involves three parcels, namely the natural convection from the heating surface to the fluid, the bulk convection induced by bubble growing and detachment and the vapour convection directly transferred into the bubble from the surface (Han and Griffith, 1962). The relative importance of these parcels depends on the thermophysical properties of the working fluids, on the geometry of the system and on bubble dynamics, which affects the convective flow and naturally, the parcel of latent heat. On of the most popular strategies to improve pool boiling heat transfer is altering surface topography, based on the argument that it increases the liquid-solid contact area and promotes the appearance of active nucleation sites within the heterogeneous nucleation process (*e.g.* Corty and Foust, 1955). While the first is an obvious benefit, the latter is not so straightforward. In fact, a larger number of active nucleation sites should promote the bulk convection induced by bubble detachment and the vapour convection, but it also endorses several interaction mechanisms between nucleation sites, which may enhance or actually inhibit it, so that the negative effects of such interaction can overcome the potential advantages. These interactions are particularly intense at high heat fluxes, which are the main target in the cooling of high energy density systems. Nevertheless, apart from pioneering work of Chekanov (1977), Sultan and Judd

(1985) and more recently Zhang and Shoji (2003), the interaction mechanisms are still sparsely reported in the literature. The relation between the dimensionless cavity spacing $S/\overline{D_b}$ - i.e. the ratio of the cavity spacing to the average bubble departure diameter and the average bubble departure frequency $\overline{f_b}$ were the parameters used to identify the different interaction regions. The most unifying theory was proposed by Zhang and Shoji (2003) who associated the interaction regions, also as a function of $S/\overline{D_b}$, with the relative importance of three competitive effects, namely the hydrodynamic interaction between bubbles, the thermal interaction between nucleation sites and the horizontal and declining bubble coalescence. The main limitation of these studies is the very restricted number of cavities which turns difficult any extrapolation to the rough surfaces used in practical applications, which have numerous cavities. In this context, the present work stands for the use of various micro-cavities.

Recent studies, based on a limited number of micro-cavities (*e.g.* McHale and Garimella, 2010, Moita *et al.*, 2011) allowed to relate the decline of the heat transfer coefficient observed at high heat fluxes (but still away from the Critical Heat Flux conditions) with the formation of large vapour bubbles, induced by the occurrence of horizontal coalescence among nucleation sites. These large bubbles cover the surface causing the decline the heat transfer, due to the low thermal conductivity of vapour and to the fact that they reduce the induced liquid motion. This suggests that especially for higher heat fluxes, an optimal pattern of the structural elements can be obtained, which besides augmenting the liquid/solid contact area, keeps the inhibitive interaction among nucleation sites under acceptable intensity, thus ensuring an overall improved cooling performance. This may be so, since in recent work, Nimkar *et al.* (2006) suggests the establishment of an optimum inter-cavity spacing, for which most of the surface remains active for a wide range of heat fluxes, although the authors are not very clear on the arguments sustaining this optimum spacing.

In this context, the present work addresses a detailed study of boiling on surfaces with a known and well defined number of artificially created cavities, to quantify the effect of the surface topography on the interaction mechanisms, and particularly on the horizontal coalescence. Special emphasis is given to understand how the interaction mechanisms affect bubbles dynamics and consequently the various parcels of the pool boiling heat transfer, as identified by Han and Griffith (1962). Understanding the flow induced by the bubbles motion is vital, since Han and Griffith (1962), who were the few authors to perform this kind of analysis, report that the convection induced by bubble motion may represent a relative importance of nearly 80%, comparing to the latent heat and to the natural convection parcels.

Few studies in the literature confirm the potential of using PIV to measure bubble velocity inside a flowing fluid, as for example reported by Sasaki *et al.* (2003) and by Cheng *et al.* (2005), although they focused mostly on the characterization of the plume, far away from the surface. In the present work, bubble detachment and induced convection velocities are investigated using PIV, at different distances from the surface. Besides the highly non uniform characteristics of boiling flows which turn them difficult to describe (particularly with PIV, which is very sensitive to them), tone challenge to overcome was to establish the measurement planes which are close enough from the surface, to provide information to be related to the bubbles detachment, while assuring the required measurements accuracy.

2. Experimental approach

2.1 Experimental set-up

The experimental arrangement mainly consists on a power supply, a heating block, a pool boiling test section, a high-speed camera (Phantom v4.2 from Vision Research Inc., with 512x512pixels@2100fps and a maximum frame rate of 90kfps) and a temperature acquisition system. Backlight illumination is provided by a 450W LED spotlight, passing through a diffusing glass to homogenize the background light. Type-K thermocouples are used to monitor and acquire the temperature and evaluate the heat flux. The signals of the thermocouples are sampled with a National Instruments DAQ board plus a BNC2120 and amplified with a gain of 300 before processing. The acquisition frequency is 100Hz and the temperature is monitored for 20 seconds after reaching a stable condition of the system that in this case has been represented by a constant temperature variation of ±0.5°C. The heating module consists on a copper support, insulated by fiberglass and heated by two electric cartridge heaters. The temperature distribution of the copper support has been evaluated by means of temperature measurements with a range of imposed heat flux. The heat losses evaluated for this configuration are 37% in the worst case. The micro-textured surfaces are placed on the top of the copper support. These surfaces, which have an area of 1cm^2, are made from silicon wafers with a thickness of 380 μm. The boiling section is directly built over the copper support. It has an area of 7.05cm^2 and a height of 15mm. The amount of liquid is 7ml. Detailed description of the experimental set-up is provided in Moita *et al.* (2012a).

The patterns are custom made, combining wet etching with plasma etching. The size and depth of the cavities was fixed for this part of the study. So, the length of the squares is 20 μm and the depth of the cavities is 30 μm. The distance between the centers of the cavities S, is the variable and ranges between 200 μm<S<2000 μm. These quantities, which are defined in Figure 1 are measured directly from the roughness profiles, obtained using a mechanical profile meter, with a measurement precision of ±100Angstroms. The main topographical characteristics of the surfaces used here are summarized in Table 1.

2.2 Characterization of the micro-textured surfaces

From the numerous patterns which were custom made to determine the effect of the surface topography in the boiling mechanisms, the surfaces used in this study were micro-textured with square cavities.

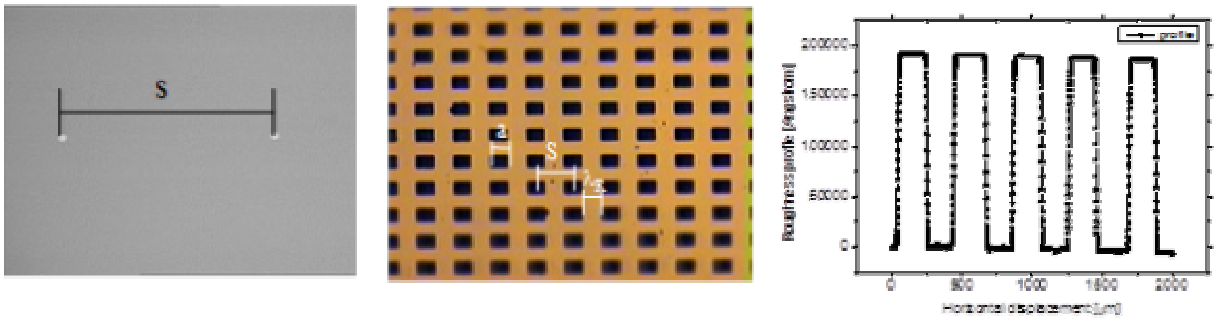

a) **b)**

Fig. 1. a) Detail of a micro-textured surface, showing the definition of the dimensions a, λ_R and S characterizing its topography. h_r is the depth of the cavities, which can be evaluated from the roughness profile, illustrated in **b)**.

Table 1. Summary of the main range of the topographical characteristics used in the customized micro-textured surfaces. Nc_{av} is the number of cavities in the entire surface.

Material	Reference	a [μm]	h_R [μm]	S [μm]	λ_R [μm]	N_{cav}
Silicon Wafer	Smooth	≈ 0	≈ 0	≈ 0	≈ 0	≈ 0
	C1	204	30	464	260	441
	C2	286	30	626	340	256
	C3	127	30	304	177	1089
	C4	52	20	400	452	625
	C5	52	20	700	752	196
	C6	52	20	800	852	144
	C7	52	20	1200	1252	64

2.3 Methodology and working conditions

The pool boiling is investigated for different liquids, namely the ethanol and water, to account for the liquid properties as well as to infer on the additional effects of wettability in the observed phenomena. Table 2 depicts the thermo-physical properties of the liquids used in the present study.

Table 2. Thermo-physical properties of the liquids used in the present study, taken at saturation, at $1.013*10^5$ Pa.

Property	Ethanol	Water
T_{sat} [°C]	78.4	100
ρ_l [kg/m^3]	736.4	957.8
ρ_v [kg/m^3]	1.647	0.5956
μ_l [mN m/s^2]	0.448	0.279
C_{pl} [J/kgK]	3185	4217
k_l [W/mK]	0.165	0.68
h_{fg} [kJ/kg]	849.9	2257
σ_{lv} [N/m] x10^3	17	58

Heat flux and heat transfer coefficients are determined for the various liquid/surface pairs. Afterwards, they are related to the bubble dynamics, which is quantified by the bubble departure diameter and frequency, active nucleation sites density, bubble growth rates and bubble velocities. This characterization is made by combining high-speed visualization with PIV measurements. To quantify the effect of horizontal coalescence, several dimensionless parameters are used, which were introduced in a previous study of the authors (*e.g.* Moita *et al.* 2012b).

Each boiling curve presented for every liquid and every heating surface used here are averaged from seven experimental curves. The curves are obtained by varying the imposed heat flux in steps of 15W/cm^2. The temperature measurements are taken for each heat flux step when the system is considered to attain equilibrium, i.e. when the temperature oscillation is ±0.5 °C. Before each experiment, the liquid is degassed by maintaining it in the pool 20°C above the saturation temperature.

Experiments were conducted to obtain average boiling curves by both increasing and decreasing the heat flux, to infer on hysteresis effects, as pointed for instance by Mohamed and Bostanci

(2002). The temperature measurements have an uncertainty of ±1°C. The relative error associated with the determination of the heat transfer is 0.014 % for the configuration using the glass surfaces coated with the Indium Oxide film and 5% for the configuration with the copper block heated by the electrical cartridge heaters.

Bubble dynamics - Image analysis procedure

Following the approach presented in the most of the works reported in the literature, the bubble nucleation parameters selected in the present study are the bubble departure diameter, the bubble departure frequency and the active nucleation sites density. This characterization is based on high-speed visualization and image post-processing. The images are recorded with a frame rate of 2200fps. For the optical configuration used here, the spatial resolution is 9.346μm/pixel.

The bubble departure diameter is measured for each test condition from 300 to 1060 frames, which were recorded at 2200 fps. For each image a mean value is averaged from 5-16 measurements for every nucleation site that is identified in the frame.

At higher heat fluxes, the various interaction mechanisms, which will be discussed in the following section, may alter significantly the value of the departure diameter, especially when horizontal coalescence occurs. Therefore, in those cases, the measured diameters are a mean value taken from the averaged diameters, which are evaluated after the occurrence of such events and the one evaluated without taking into account such events.

The error associated to the measurements of the bubble departure diameter is of ±1 pixel, corresponding to ±9.346 μm.

The bubble departure frequency is estimated by determining the time elapsed between apparent departure events, which are counted for a defined interval of time. The departure frequency is assessed, for each test condition, for at least five nucleation sites, which are evaluated based on extensive image post-processing of 300 to 1060 frames, which were recorded with a frame rate of 2200fps. The final value of the bubble departure frequency is the average between the frequencies of each nucleation site. The uncertainty associated to these measurements is ±1 fps.

Finally, the evaluation of the active nucleation sites density must be done by visual inspection of the frames, which introduces an uncertainty associated to the subjective criterion of the observer. To lessen this uncertainty, at least ten frames are chosen, at different times during the single experiment. The final values of the active nucleation site density are an average of the ten evaluated values. The uncertainty introduced in the visual identification of the nucleation sites by the chaotic behaviour of the boiling phenomenon was assessed in the "worst scenario" to be ±18%.

PIV measurements

Several studies in the literature confirm the potential of using PIV to measure bubble velocity inside a flowing fluid, as for example reported by Sasaki *et al.* (2003) and by Cheng *et al.* (2005). However, the results obtained from this technique are very sensitive to the characteristics of the flow and to the parameters used during the visualization and the post-processing of the images (*e.g.* Cheng *et al.*, 2005). In the present work, the main focus is to measure the velocity of the bubbles, so any kind of seeding was used, but instead the bubbles themselves are used as seeding particles, as also suggested by Cheng *et al.* (2005). The bubble diameter of ethanol is in the range of 500-800 μm, measured by image post-processing. These dimensions and the low characteristic velocities of the bubbles (1-10 cm/s) require a careful analysis of all the parameters which have to be selected in the PIV configuration. The PIV system uses a CCD camera Kodak Megaplus, Model 1.0, with an image resolution of 1018x1008 pixel^2. The bubbles are illuminated via a dual Nd:YAG Litron laser. The time delay between laser pulses is varied ($1<\Delta t<8$ms) depending on the imposed heat flux: the time between pulses is smaller for higher imposed heat fluxes. Furthermore, the interrogation area and the overlap are also varied for the various imposed heat flux conditions, in an optimization process, to assure that the chosen values are adequate to obtain accurate measurements. Hence, the

selected interrogation area was varied between 16 and 64 pixels (1pixel/58μm) to assure that at least five bubbles are inside. An overlap of 50% is chosen by analyzing two consecutive frames and evaluating the average displacement of the bubbles. The most appropriate approach for this kind of flow is using a recursive cross correlation or the average correlation algorithms (*e.g.* Cheng *et al.*, 2005). In the present work, after analyzing extensively both approaches, the cross correlation was considered to be the most appropriate. Figure 2 represents a typical flow field obtained. The measurements performed using PIV are compared with extensive image post-processing, within quite good agreement. The PIV data were processed with the software Flow manager 4.2.

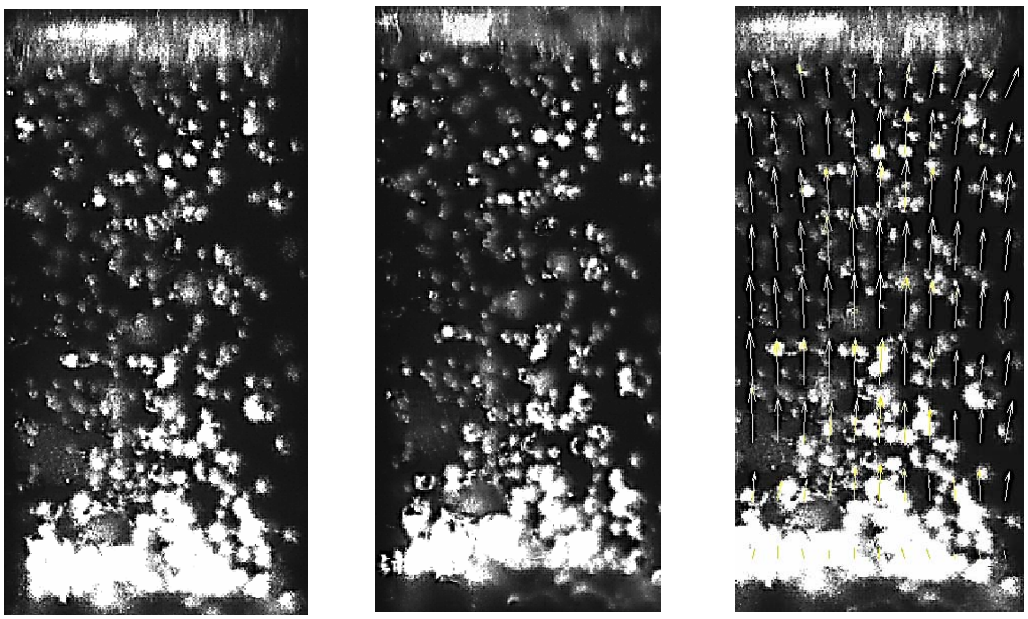

a) **b)** **c)**

Fig. 2. Example of image analysis by average cross correlation: a) Frame corresponding to the first laser pulse, b) Frame corresponding to the second laser pulse, c) Flow field obtained after applying average correlation algorithm.

3. Results and discussion

The present study is part of a work aimed at optimizing pool boiling heat transfer for cooling applications, using micro-structured surfaces. The micro-structures must be designed to optimize the heat transfer by balancing the positive aspect of the micro-cavities in increasing the number of active nucleation sites and the negative effect that horizontal coalescence introduce both in the deterioration of the heat transfer due to the increase of vapor cushion near the wall and in the possible modifications it can introduce in the convective flow induced by the bubbles. In line with this, a short summary of the quantification of the effect of the horizontal coalescence in several parameters such as the departure frequency and the convection heat transfer is introduced in the first sub-section. Then the main focus of the results presented in the subsequent sub-paragraph is in the characterization of the flow, namely on the average vertical bubble velocity, determined from PIV measurements. Finally, the third sub-paragraph relates the bubble dynamics with the bubble velocities to understand how they affect the three parcels composing pool boiling heat transfer and sub-subsequently, the convective heat transfer coefficient, for the various micro-textures.

3.1 Effects of horizontal coalescence in the global pool boiling heat transfer

Bubble dynamics was described using high-speed visualization and image post-processing to quantify characteristic quantities such as the bubble departure diameter, the departure frequency and the active nucleation sites density. There is a clear deterioration of the heat transfer coefficient

caused by overstated horizontal coalescence (*e.g.* Moita *et al.*, 2011). In this context, the coalescence factor $D^* = D_b/D_{nc}$ was introduced to quantify intensity of horizontal coalescence in the boiling of water and over various micro-textured surfaces. The coalescence factor, defined by the ratio between the average bubble departure diameter (including coalescence) and the single diameter of the bubbles which exit the cavity with no coalescence is usually larger than 1 for liquids with large surface tension and very close to 1 for liquids with smaller surface tension. Hence, strong coalescence occurs during water boiling in opposition to ethanol. Additionally, the distance between the cavities S can promote coalescence. Against intuition, the coalescence factor does not increase as S decreases. Instead, there is an optimum range, which is naturally different depending on the liquid surface tension (*e.g.* Moita *et al.*, 2012b). Further introducing the departure frequency as a variable, it is clear that there is a maximum value of f_d, which can be related to an optimum distance S, which keeps the coalescence under controlled activity. Finally, the active nucleation sites density must also be considered as it introduces the relative importance of the latent parcel of heat removed during vaporization. An extensive analysis of these parameters is out of the scope of the present paper, but can be found in Moita *et al.* (2012b). However, such analysis which is currently in progress, suggests that an optimum spacing to balance the occurrence of coalescence with the promotion of active nucleation sites can be identified based on the map depicted in Fig. 3. This map represents the heat transfer performance of a structured surface, referenced to the smooth one, as the ratio between the average heat transfer coefficients h_{av}/h_{smooth}, with the dimensionless distance S/L_c, in which L_c is the characteristic length scale from Fritz's equation (Chaptun *et al.*, 2004), $L_c=(\sigma_{lv}/g(\rho_l-\rho_v)^{1/2}$, where g is the gravitational constant and ρ_l and ρ_v are the liquid and vapor specific masses, respectively.

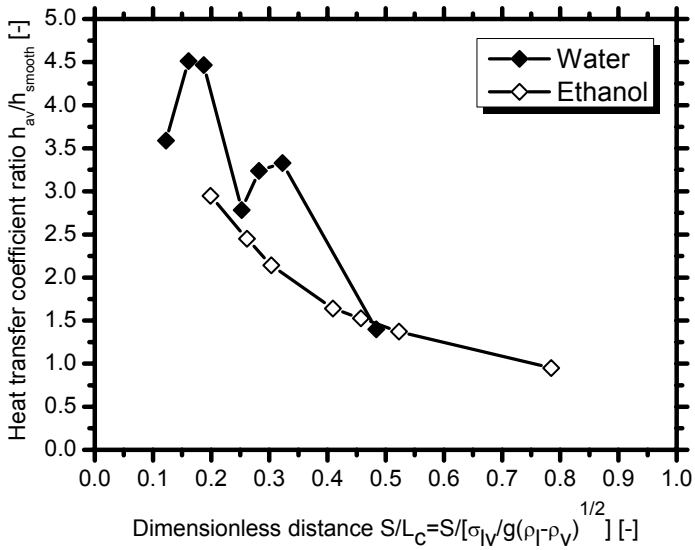

Fig. 3. Heat transfer ratio versus dimensionless distance for water and ethanol in the range of the patterns studied.

For the fluid with the lowest surface tension (ethanol), the map is not well established yet as we have not reached the ranges of the patterns required achieving a maximum, although it should within a range close to 300-400μm. On the other hand, for water, one can identify two peaks: the maximum occurring at $0.15<S/L_c<0.18$ and a lower one identified at $0.31<S/L_c<0.37$. The highest peak corresponds to the patterns with the S around 400μm, while the second corresponds to S between 700 and 800μm.

3.2 Flow description: analysis of the average vertical bubble velocity

The effect of surface topography on bubble size and frequency clearly affects the heat transfer coefficient, due to the formation of large vapor bubbles. These modifications, induced in bubble size and frequency are expected to alter the bubbles' velocity, which in turn will affect the induced convection. This effect was investigated evaluating the average vertical bubble velocity (average of the velocity profile for a fixed value of H/D), along the vertical dimensionless distance H/D, where H is the vertical distance from the top face of the surface in (mm) and D is the bubble departure diameter (also in mm), for different heating conditions and different micro-textures. Here one will start from the smooth surface and then will progressively increase the number of cavities (i.e., decreasing S). From the analysis performed in the previous sub-section, three representative micro-textures were selected: the one with the largest distance between cavities (S=1200μm), one with intermediate distance, identified by the lower maximum in Fig. 3 (S=800μm) for the water and the best performing structure, identified by the maximum for water in Fig. 3 (S=400μm), which is also one of the best performing surfaces for ethanol.

Hence, starting with the smooth surface, which is taken as a reference, Table 3 depicts the detailed characterization of the measurements made. From the left side, first columns present the heat transfer parameters (T_w-T_{sat}, heat flux and heat transfer coefficient). The characteristic velocity obtained with PIV measurements (i.e. the value of the velocity in the vertical position where the bubble reaches the constant velocity) is presented in the 5th column. Finally, some of the relevant parameters set for the PIV configuration are shown, namely the time between laser pulses t_{bp}, the correlation type, the side of the interrogation area I.A and the overlap used.

Table 3. Complete panoramic of all the characteristics and main PIV parameters for the smooth surface.t_{bp} is the time between pulses and I.A is the interrogation area.

N°	T_w-T_{sat} [-]	Heat flux [W/cm^2]	Heat transfer coefficient [W/cm^2K]	Bubble departure diameter D[mm]	Characteristic velocity $V_{H/D=10-20}$ [cm/s]	t_{bp} [ms]	Corr. Type	I.A [Px]	Overlap %
1	30.3	35.91	1.186582	1.26	8.9	3	cross	64	50
2	26.5	30.16	1.139484	1.19	7.47	3	cross	64	50
3	24.7	29.66	1.192216	1.21	5.86	3	cross	64	50
4	15.4	18.09	1.205537	0.99	4.65	5	cross	64	50
5	17.8	20.89	1.187963	1.19	3.9	3	cross	64	50
6	10.8	10.54	0.955608	0.78	2.52	5	cross	64	50
7	7.5	8.11	1.053937	0.74	2.02	8	cross	64	50
8	2.5	1.79	0.84079	0.72	1.44	8	cross	64	50

Fig. 4 depicts the average vertical velocity of the bubble versus the dimensionless distance H/D, for different heating conditions, for the pool boiling of ethanol on the smooth surface. Starting from H/D≈0 (top face of the heating surface), the bubble velocity increases until reaching an almost constant value which remains stable for increasing values of H/D. A slight increase of the vertical velocity occurs for 10<H/D<18 as one increases the imposed heat flux and then decelerates due to the braking effect imposed by the zero velocity at the top of the pool. As the imposed heat flux is higher, the bubbles are ejected with larger average velocity but then quickly slow down, since the plume becomes wider so this breaking effect starts to occur at lower values of H/D. Due to the small number of nucleation sites on the smooth surface, the interaction among them is negligible, so the vertical velocity is not much disturbed. This explains the constant value observed for the wide range of H/D.

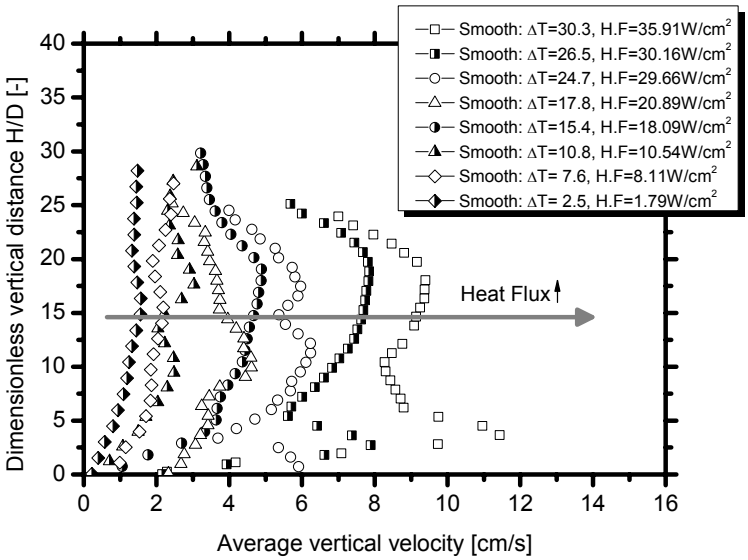

Fig. 4. Average vertical velocity versus dimensionless vertical distance for the pool boiling of ethanol on the smooth surface. Here, $\Delta T = T_w - T_{sat}$ and H.F. is the imposed heat flux.

The first structured surface to be analyzed is the one with the largest distance among cavities, thus with the smallest number of cavities (surface C7, S=1200μm). Table 4 summarizes the relevant parameters for the analysis of the results. Here, 5th and 6th columns add the bubble departure frequency and the product $f_d D_b$, which could not be accurately determined for the smooth surface given the very small number of active nucleation sites. $f_d D_b$ provide a sort of reference value for the velocity, which is actually quite close to those obtained from the PIV measurements, particularly for lower imposed heat fluxes. This good agreement between $f_d D_b$ and the average vertical velocity confirms the reliability of the measurements.

Table 4. Complete panoramic of all the characteristics and main PIV parameters for surface C7 (S=1200μm).t_{bp} is the time between pulses and I.A is the interrogation area.

N°	T_w-T_{sat} [-]	Heat flux [W/cm^2]	Heat transfer coefficient [W/cm^{2}K]	Bubble departure diameter D[mm]	Bubble departure frequency f_d [Hz]	$f_d D_b$ [cm/s]	Characteristic velocity $V_{H/D=10-20}$ [cm/s]	t_{bp} [ms]	Corr. Type	I.A [Px]	Overlap %
1	24.2	23.65	0.96	0.89	80	7.12	14.71	5	Average	64	50
2	20.5	20.35	1.01	0.85	81	6.88	11.45	2	Cross	64	50
3	17.5	18.35	1.02	0.8	90	7.20	8.3	2	Cross	64	50
4	18.2	19.35	1.01	0.82	89	7.29	6.83	2	Cross	64	50
5	13.2	13.45	0.95	0.63	83	5.22	7.65	2	Cross	64	50
6	12.1	11.54	0.91	0.57	82	4.67	6.59	3	Cross	64	50
7	13.5	13.88	0.98	0.64	83	5.31	4.4	3	Cross	64	50
8	8.5	8.68	0.98	0.39	79	3.08	3.99	3	Cross	64	50

The average vertical bubble velocity versus the dimensionless distance H/D obtained for the pool boiling of ethanol on surface C7 (S=1200μm) is depicted in Fig. 5, for various imposed heat fluxes.

The presence of preferential nucleation sites on the surface increases the complexity of the phenomena involved and thus of the analysis. In this case one can only evidence the fact that the velocity increases with the heat flux. The evolution with H/D is far more difficult to explain since the average velocity starts to increase from H/D=0 up to H/D=10 and then assumes a constant value, as for the smooth surface. However, in this case, strong oscillations of the velocity occur

around this average value, between 10<H/D<20. The magnitude of these oscillations increases with the heat flux. These oscillations are attributed to some interaction phenomena which can already exist. The horizontal coalescence is not much strong but interaction between nucleation sites already exists, which increases the size of the bubbles and decreases the departure frequency. This effect allied to the interaction between raising bubbles turns the boiling process much more chaotic, when compared to the smooth surface. Consequently, bubbles motion is much more random and affects negatively the convective motion of the flow. Hence, contrarily to expectations, this surface is slightly underperforming in terms of heat transfer, when compared to the smooth surface, which can be noticed by comparing the values of the heat transfer coefficient in Tables 3 and 4.

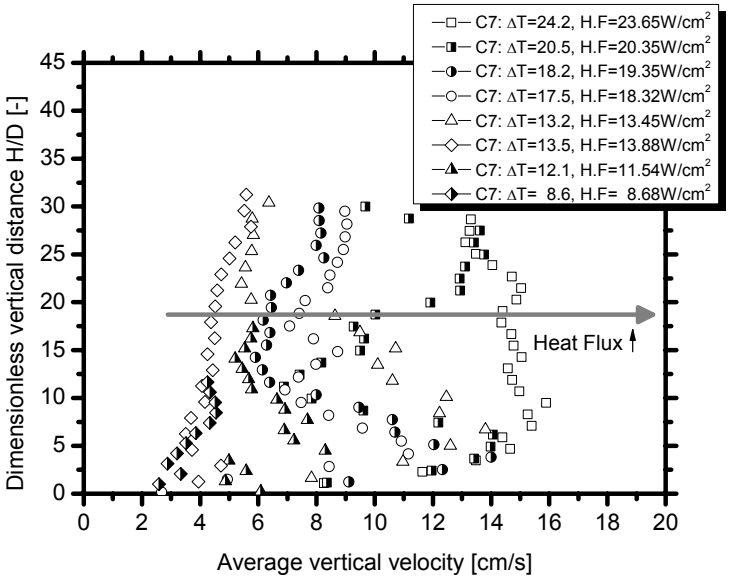

Fig. 5. Average vertical velocity versus dimensionless vertical distance for ethanol on the surface C7 (S=1200μm). $\Delta T = T_w - T_{sat}$ and H.F is the imposed heat flux.

Further decreasing the distance between cavities to S=800μm (surface C6), one may notice that the order of magnitude of the reference velocity $f_d D_b$ and the characteristic velocity is really similar. Once again, the most relevant parameters for the analysis are summarized in Table 5.

Table 5. Complete panoramic of all the characteristics and main PIV parameters for surface C6 (S=800μm). t_{bp} is the time between pulses and I.A is the interrogation area.

N°	T_w-T_{sat} [-]	Heat flux [W/cm^2]	Heat transfer coefficient [W/cm^{2}K]	Bubble departure diameter D[mm]	Bubble departure frequency f_d [Hz]	$f_d D_b$ [cm/s]	Characteristic velocity $V_{H/D=10\text{-}20}$ [cm/s]	Tbp [ms]	Corr. Type	I.A [Px]	Overlap %
1	16.2	24.72	1.50	0.82	74	6.06	12.82	1	Cross	64	50
2	13.7	18.48	1.35	0.81	73	5.91	10.61	1	Cross	64	50
3	22.3	36.03	1.60	0.84	77	6.46	8.81	1	Cross	64	50
4	24.4	39.70	1.59	0.84	75	6.31	6.15	2	Cross	64	50
5	20.6	28.23	1.38	0.84	76	6.38	5.53	1	Cross	64	50
6	5.3	5.56	1.24	0.75	65	4.87	3.3	1	Cross	64	50
7	4.2	4.91	1.04	0.74	62	4.58	2.97	2	Cross	64	50
8	2.2	2.34	1.01	0.72	59	4.24	2.29	2	Cross	64	50

Similarly to what was observed with the previous surfaces, the velocity increases for H/D=0 up to 10<H/D<20. Then, the trend of the characteristic velocity is quite dependent on the imposed heat fluxes, as shown in Fig. 6.

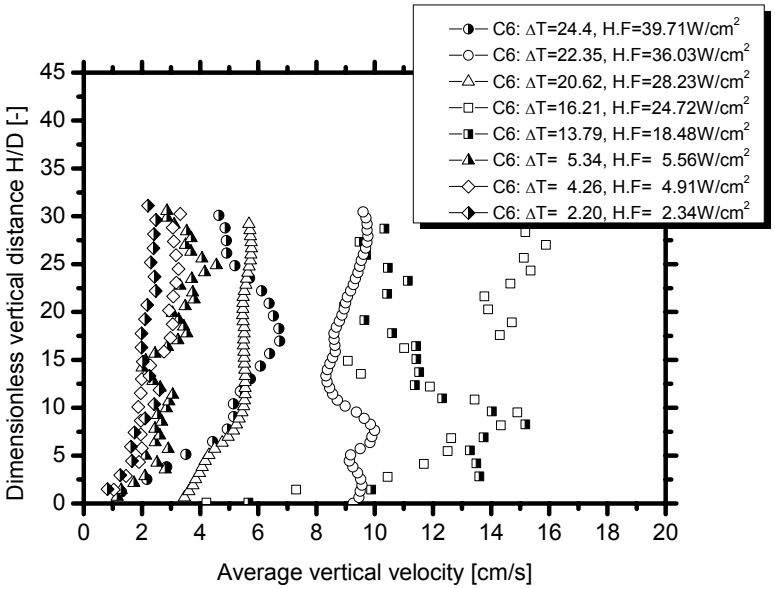

Fig 6. Average vertical velocity versus dimensionless vertical distance for ethanol on the surface C6 (S=800μm). $\Delta T = T_w - T_{sat}$ and H.F is the imposed heat flux.

Hence, for this surface, the characteristic velocity is observed to stabilize around a constant value, for the lowest and for the highest imposed heat fluxes. Instead, for intermediate values of the heat fluxes, one may observe larger characteristic velocities, which are however affected by stronger oscillations. These oscillations are no longer random and seem to be stabilized for higher heat fluxes, when the interaction mechanisms are stronger. It is argued that with the stronger interaction mechanisms, much more intense boiling process promotes mixing but also allows the formation of defined bubble columns in which subsequently detached bubbles are dragged, thus promoting a convective motion. Hence, one may argue that besides being an optimal distance between cavities, which will balance the positive effect of the larger number of cavities with a stronger horizontal coalescence, there is also an optimum distance which will actually stabilize the boiling process. In this case, the process is already stable at the lowest and highest imposed heat fluxes (the result for the lowest heat flux is obviously due to a negligible interaction effect, but the highest may be already attributed to the aforementioned stabilizing effect).

To confirm this trend, one will further decrease S to 400μm, for which the most relevant parameters are summarized in Table 6.

The stabilizing effect of the interaction is very clear with this surface, as shown in Fig. 7: the velocity for increasing values of H/D is well defined for all the heat fluxes, thus after the initial increase of the characteristic velocity for H/D>0, which is related to the detachment of the bubbles, there is an extended range of 7.5<H/D<15 for which the characteristic velocity remains constant, with no significant oscillations. The high heat transfer rates promoted by this surface (which were already identified in Fig.3) promote very fast evaporation so the braking effect which occurs as the bubbles reach the top of the pool is now more evident, as the velocity starts to decrease at lower values of H/D.

In summary, the effect of surface topography seems indeed to be strongly related to interaction mechanisms. There is however an optimum pattern which promotes stable convective motion, while others, for which the distance between cavities is not adequate, may actually destabilize the bubble motion leading to an inefficient heat transfer process.

This is clearly understood by relating the thermal characteristics with the bubble velocity, as discussed in the following sub-paragraph.

Table 6. Complete panoramic of all the characteristics and main PIV parameters for surface C4 (S=400µm). t_{bp} is the time between pulses and I.A is the interrogation area.

N°	T_w-T_{sat} [-]	Heat flux [W/cm^2]	Heat transfer coefficient [W/cm^{2}K]	Bubble departure diameter D[mm]	Bubble departure frequency f_d [Hz]	f_dD_b [cm/s]	Characteristic velocity $V_{H/D=10-20}$ [cm/s]	Tbp [ms]	Corr. Type	I.A [Px]	Overlap %
1	24.8	42.37	1.7	1.02	50.33	5.17	6.07	2	Cross	64	50
2	19.1	35.06	1.83	1.02	31.30	3.19	5.32	2	Cross	64	50
3	15.5	29.54	1.91	1.03	37.50	3..88	5.27	2	Cross	64	50
4	22.2	39.343	1.76	1.02	38.46	3.95	4.94	1	Cross	64	50
5	15.7	30.93	1.89	0.92	36.75	3.38	4.67	1	Cross	64	50
6	14.3	28.1	1.93	0.92	42.89	3.94	3.97	1	Cross	64	50
7	17.2	33.04	1.86	1.03	32.59	3.36	3.63	2	Cross	64	50
8	7.9	17.04	2.07	0.75	81.16	6.08	2.73	1	Cross	64	50

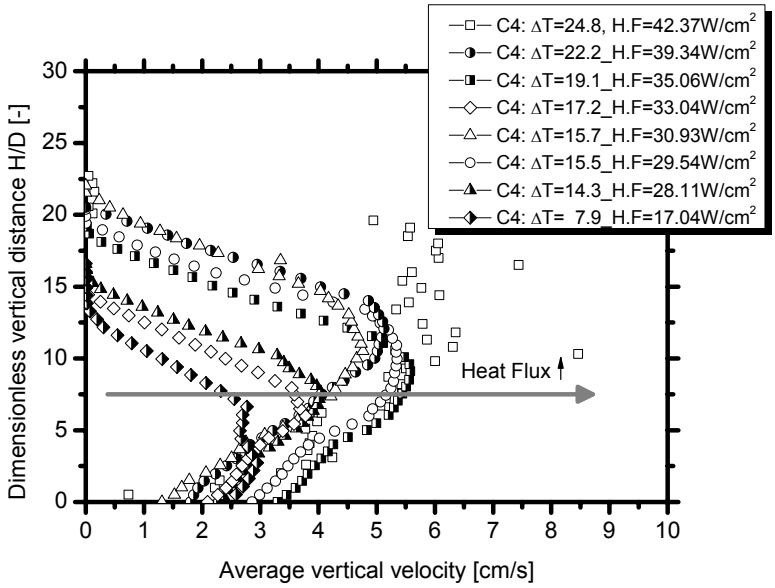

Fig 7. Average vertical velocity versus dimensionless vertical distance for ethanol on the surface C4 (S=400µm). $\Delta T = T_w - T_{sat}$ and H.F is the imposed heat flux.

3.3 Relation between the micro-texture, the thermal characteristics and the bubble velocity

Fig. 8 relates the bubble characteristic velocity $V_{H/D=10-20}$ with the wall superheat for the four surfaces studied. The meaning of the characteristic velocity is to identify the value of the velocity that the bubble reaches when it starts to oscillate around a constant value, thus for 10<H/D<20. The velocity increases with wall superheat and therefore with the imposed heat flux for all the surfaces, exception made to surface C6 (S=800µm). This is evident since the higher superheat will promote larger temperature differences between the surface and the liquid, which in turn will lead to larger density differences between the liquid near and far from the wall, thus promoting natural convection. Surprisingly, the best performing surface in terms of heat transfer coefficient and in terms of velocity stabilization (surface C4, S=400µm) is the one leading to the lowest bubble velocity. This may be due to the fact that with this surface, the optimization process of defining the spacing S is not precluding horizontal coalescence, but balancing it, to avoid fast heat transfer deterioration due to the formation of very large vapor bubbles. However, further investigation is still required to explain this, even because these coalescence phenomena occur very close to the surface, so one must deal with the known, but yet very debated issues of measurement accuracy within this region.

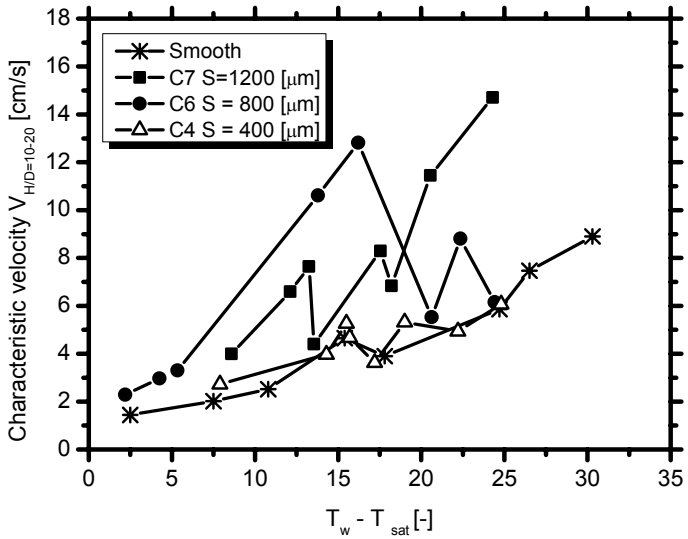

Fig 8. Characteristic velocity versus wall superheated for the surfaces studied during the work.

So, the convection induced by bubble motion is actually quite reduced with this surface, as shown in Fig. 9, which evidences the decrease of the heat transfer coefficient with the characteristic velocity.

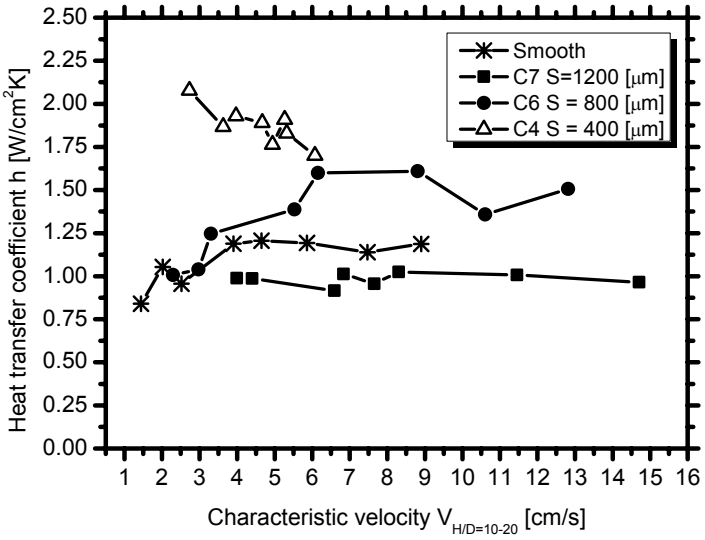

Fig. 9. Heat transfer coefficient versus characteristic velocity for the surfaces studied in this work.

The relation between the characteristic velocity and the heat transfer coefficient is not straightforward since the heat transfer coefficient is a complex function of many parameters related to bubble dynamics, flow motion and interaction mechanisms, which affects the three parcels identified by Han and Griffith (1962). Additional complexity arises from the use of structured surfaces, which will affect the various aforementioned parameters, in different ways. However, from the whole analysis reported here one may argue that the optimization of bubble dynamics and coalescence indicates preferential patterns. Then, additional information can be inferred from bubble velocity. In fact the best performing pattern identified by the analysis of bubble dynamics and coalescence provide stable bubbles motion. Nevertheless, their velocity is quite low, so the convection induced by bubble motion is reduced in this surface. In line with this, one may argue

that the positive effect of increasing nucleation sites (under controlled coalescence) considerably improves the latent heat parcel, which is dominant mechanism, contrarily to the cases studied by Han and Griffith (1962). The fact that it promotes the stability of the vertical velocity may also be positive in removing the vapor away from the surface. The dominant effect of this parcel also seems plausible, since the surface promoting the largest velocities (C7, S=1200μm) had the lowest heat transfer coefficient, given the lowest number of active nucleation sites. Additionally, destabilization of the bubbles velocity was induced, which would actually contribute to the deterioration of the heat transfer coefficient.

The analysis presented here is yet preliminary, but suggests that the optimization of the surface topography for pool boiling heat transfer enhancement can be achieved by combining bubble dynamics, flow dynamics and heat transfer analysis. Image analysis combined with PIV is proposed as a good approach to perform this task efficiently.

4. Final remarks

The present work addresses a detailed study on the pool boiling processes on surfaces with a known and well defined number of artificially created cavities, to quantify the effect of the surface topography, on the interaction mechanisms. Understanding the flow induced by the bubbles motion is vital, since Han and Griffith (1962) report that the convection induced by bubble motion may represent a relative importance of nearly 80%, comparing to the other two parcels. In this context, an innovative analysis of the boiling process from structured surfaces is proposed here, which combines image post-processing with PIV measurements.

The results show that the characterization of the bubble dynamics by image analysis allows identifying optimum micro-textures which balance the effect of promoting activation of nucleation sites with a controlled activity of horizontal coalescence, thus effectively enhancing the pool boiling heat transfer. Analysis of the characteristic bubbles velocity obtained by PIV measurements evidences that optimal patterns controlling horizontal coalescence (with a distance between cavities S=400μm) allow a more stable vertical bubble velocity, thus removing the vapour from the surface. However, the velocity of the bubbles for these surfaces is quite low, when compared to that of surfaces with a smaller number of cavities, i.e., with larger S. Hence, the convection induced by bubble motion is reduced in these optimal patterned surfaces, although the heat transfer coefficient is the highest. In line with this one may argue that the positive effect of increasing nucleation sites (under controlled coalescence) considerably improves the latent heat parcel, which is dominant. This may be so, since the surface pattern promoting the largest velocities (C7, S=1200μm) has the lowest heat transfer coefficient, given the lowest number of active nucleation sites. Additionally, destabilization of the bubbles velocity is induced in this surface, which would actually contribute to the deterioration of the heat transfer coefficient.

The analysis presented here is yet preliminary, but suggests that the optimization of the surface topography for pool boiling heat transfer enhancement can be achieved by combining bubble dynamics, flow dynamics and heat transfer analysis. Image analysis combined with PIV is proposed as a good approach to perform this task efficiently.

5. Acknowledgements

The authors are grateful to Fundação para a Ciência e a Tecnologia (FCT) for partially financing the research under the framework of project PTDC/EME-MFE/109933/2009 and for supporting E. Teodori with a research grant. A.S. Moita also acknowledges the contribution of FCT by supporting her with a Fellowship (Ref.:SFRH/BPD/63788/2009).

References

Calka, A., Judd, R. L. (1985) Some aspects of interaction among nucleation sites. Journal of Heat Transfer – Transactions of the ASME, 102(3):461-464.

Chaptun S., Watanabe M., Shoji M. (2004) Nucleation site interaction in pool nucleate boiling on a heated surface with triple artificila cavities. Int. J. Heat Mass Transf., 47:3583-3587.

Chekanov, V. (1977) Interaction of centers during nucleate boiling. Teplofizika Vysokikh Temperature, 15:121-128.

Cheng, W. Murai, Y., Sasaki, T. Yamamoto, F. (2005) Bubble velocity measurement with a recursive cross correlation PIV technique. Flow Measurement and Instrumentation, 16:35–46.

Corty C., Foust, A. S. (1955) Surface variables inn nucleate boiling. Chem.Eng.Progress.Symo Ser. 51(17):1-12.

Han, C. Y., Griffith, P. (1962) The mechanism of heat transfer in nucleate boiling. Technical Report No 7673-19, Dep. Mech. Eng., M.I.T.

McHale J. P.,Garimella S. V. (2012) Bubble nucleation characteristics in pool boiling of wetting liquid on smooth and rough surfaces, Int. J. Multiphase Flow, 36:249-260, 2010.

Mohamed, S. E., Bostanci, H. (2002) Thermal Challenges in Next Generation Electronic Systems. Joshi & Garimella (Eds), Millpress, Rotterdam, ISBN 90-77017-03-8.

Moita A. S.,Teodori, E., Moreira, A. L. N. (2011) Influence of surface topography and wettabiblity in the boiling mechanisms, ILASS 24th Annual Conference on Liquid Atomization ans Spray Systems – ILASS2011, Estoril, Portugal.

Moita, A. S., Teodori, E., Moreira, A. L. N. (2012a) Influence of the surface topography in the boiling mechanisms. Submitted to the Int. J. Heat Fluid Flow.

Moita, A. S., Teodori, E., Moreira, A. L. N. (2012b) Enhancement of pool boiling heat transfer by surface micro-structuring. To be presented at the 6th European Thermal Science Conference, Eurotherm 2012-03-28.

Nimkar D. N., Bhavnani S. H., Jaeger R. C. (2006) Effect of nucleation sites spacing on the pool boiling characteristics of a structured surface, Int. J. Heat Mass Transf., 49:2829-2839.

Zhang, L., Shoji, M. (2003) Nucleation sites interaction in pool boiling on the artificial surface. Int. J. Heat Mass Transf., 46(3):513-522.